



A Journal of the Gesellschaft Deutscher Chemiker

Angewandte Chemie

GDCh

International Edition

www.angewandte.org

Accepted Article

Title: Fullerene-Based Molecular Torsion Balance for Investigating Noncovalent Interactions at C60 Surface

Authors: Michio Yamada, Haruna Narita, and Yutaka Maeda

This manuscript has been accepted after peer review and appears as an Accepted Article online prior to editing, proofing, and formal publication of the final Version of Record (VoR). This work is currently citable by using the Digital Object Identifier (DOI) given below. The VoR will be published online in Early View as soon as possible and may be different to this Accepted Article as a result of editing. Readers should obtain the VoR from the journal website shown below when it is published to ensure accuracy of information. The authors are responsible for the content of this Accepted Article.

To be cited as: *Angew. Chem. Int. Ed.* 10.1002/anie.202005888

Link to VoR: <https://doi.org/10.1002/anie.202005888>

RESEARCH ARTICLE

Fullerene-Based Molecular Torsion Balance for Investigating Noncovalent Interactions at C₆₀ Surface

Michio Yamada,^{*[a]} Haruna Narita,^[a] and Yutaka Maeda^[a]

Dedicated to Professor François Diederich on the occasion of his retirement

[a] Prof. Dr. M. Yamada, H. Narita, Prof. Dr. Y. Maeda
Department of Chemistry,
Tokyo Gakugei University,
Nukuikitamachi 4-1-1, Koganei, Tokyo 184-8501 (Japan)
E-mail:

Supporting information for this article is given via a link at the end of the document.

Abstract: In order to investigate the nature and strength of noncovalent interactions at the fullerene surface, molecular torsion balances consisting of C₆₀ and organic moieties connected through a biphenyl linkage were designed, synthesized, and characterized. NMR spectroscopy combined with computational studies showed that the unimolecular system remains in equilibrium between well-defined folded and unfolded conformers owing to restricted rotation around the biphenyl C–C bond. The measured energy differences between the two conformers depend on the substituents and can, in turn, be ascribed to the differences in the intramolecular noncovalent interactions between the organic moieties and the fullerene surface. Notably, the results showed that fullerenes favor interacting with the π -faces of benzenes bearing electron-donating substituents. The correlation between the folding free energies and the corresponding Hammett constants of the substituents in the arene-containing torsion balances is reflective of the contributions of the electrostatic interactions and dispersion force to the face-to-face arene–fullerene interactions.

Introduction

Fullerenes are unique molecules with spherical hydrophobic structures and curved π -electron systems, and are expected to find widespread use in a variety of applications in the materials science and medicinal chemistry fields.^[1] Therefore, quantitative investigations of the noncovalent interactions at the fullerene surface, which are often very weak, are essential for understanding the assembled molecular systems of fullerene as well as its molecular recognition events.^[2] The fact that the fullerene molecule has a unique surface suggests the possibility of effective noncovalent interactions with aromatic and aliphatic biomolecular moieties such as proteins, nucleic acid bases, and antibiotics in biosystems. In addition, the organocatalytic activity of fullerene conjugates featuring anion– π interactions between the anionic transition states or the intermediates of the reactants and the fullerene surface have been reported.^[3] Moreover, recent studies on the supramolecular chemistry of fullerenes have shown that structurally well-defined molecular receptors exhibit strong noncovalent interactions with fullerenes to form stable complexes.^[4] In many cases, such fullerene receptors are constructed through the assembly of π -extended molecules such as porphyrins^[5] and polyaromatic hydrocarbons.^[6] It has also

been reported that porous metal–organic cages are suitable for fullerene binding.^[7] Nevertheless, determining the nature and strength of the noncovalent interactions between fullerenes and the functional groups of the organic moiety in question remains challenging because of the difficulty in observing such weak interactions and distinguishing between the various factors contributing to them.^[8,9]

The distribution of the electrostatic potentials of C₆₀ is different from that of benzene. In the case of benzene, the positive electrostatic potentials are associated with hydrogens while the negative electrostatic potentials are the strongest above and below the benzene ring. In contrast, in C₆₀, the positive electrostatic potentials are located above the pentagonal and hexagonal rings while the negative electrostatic potentials are located above the edges shared by the two adjacent hexagonal rings, as demonstrated by Wang et al.^[8d] His group also performed symmetry-adapted perturbation theory (SAPT)^[10] calculations of the noncovalent interactions between benzene and C₆₀ in the gas phase and showed that the face-to-face configurations of the benzene–C₆₀ complex are more strongly bound than the edge-to-face configurations.^[8d]

Meanwhile, noncovalent arene–arene interactions have been studied extensively.^[11–13] A key feature of the aromatic interactions is the fact that arene surfaces can exhibit a variety of geometries with similar energies. In addition, various intermolecular forces contribute equally to the arene–arene interactions. Therefore, noncovalent arene–arene interactions have become an important topic of study in computational chemistry. The pioneering work of Hunter and Sanders led to the development of a qualitative model that states that the strength and preferred orientation of the arene–arene interactions may be understood based on the aromatic quadrupole moments and the electrostatic effects of the substituents can be attributed to the polarization of the electrons in the attached aromatic ring by the substituents.^[14] Later, Wheeler and Houk introduced the local, direct-interaction model for the substituent effects in the case of face-to-face arene–arene interactions, stating that the substituent effects for these interactions are primarily attributable to the direct, through-space interactions of the substituent with the proximal vertex of the other ring.^[13f,13g]

In the 1990s, based on experimental studies, Wilcox and coworkers developed a unimolecular model system, called a molecular torsion balance, to evaluate edge-to-face arene–arene interactions using the rigid V-shaped structure of Tröger's base

RESEARCH ARTICLE

as the scaffold.^[15] Wilcox's torsion balance was designed to be in equilibrium between the well-defined folded and unfolded conformers based on restricted rotation around the biphenyl C–C bond. The conformationally flexible ester sidearm allows for the adjustment of the effective edge-to-face contacts. It has been suggested that, in Wilcox's systems, motion in the ester linkage is not an important factor with respect to folding.^[16] By analyzing the folding energies for torsion balances with different substituents, Wilcox et al. concluded that the edge-to-face arene–arene interactions are dominated by dispersion rather than by electrostatic forces.^[15] Since then, the concept of the synthetic molecular balances has been employed for investigating a range of noncovalent interactions, given their excellent applicability. Recent studies have shown that such balances allow for highly accurate and sensitive measurements of noncovalent interactions.^[17–19] For instance, Shimizu et al. assessed the additivity of the substituent effects for arene–arene interactions using a torsion balance that could adopt an offset face-to-face stacking geometry and found that the additive substituent effects were consistent with the Wheeler–Houk model.^[19] These successes motivated us to extend the idea of molecular balances to fullerenes in order to investigate the noncovalent interactions at the fullerene surface. Thus, in this study, we designed, synthesized, and characterized the first model system of a fullerene-based molecular balance to quantitatively analyze the noncovalent interactions at the C₆₀ surface.

Results and Discussion

Molecular Design and Synthesis

Figure 1 depicts the fullerene-based molecular torsion balances, **1a–1h**, designed in this study. In its folded conformation, the proposed model system features an intramolecular noncovalent interaction between the organic moiety (R) and the C₆₀ surface, which competes with solvation. However, this interaction is absent in its unfolded conformation. It is expected that ring X is positioned parallel to the fullerene surface in order to prevent steric repulsion between the aromatic protons of the ring and the fullerene surface. This hypothesis is in keeping with the results of crystallographic analyses of relevant pyrrolidinofullerenes.^[20] Moreover, Nierengarten and coworkers reported that rotation around the phenyl–pyrrolidine bond in phenyl-substituted pyrrolidinofullerenes is restricted.^[21] The neighboring ring, that is, ring Y, is preferentially perpendicular to ring X, owing to the steric repulsion between the aryl protons. Accordingly, it is expected that the organic moiety, R, which is connected with ring Y through an ester linkage, becomes close to the fullerene surface in the folded conformation, in a manner similar to that for the folded conformation of the Wilcox's torsion balance. On the other hand, it is likely that R would move away from the fullerene surface in the unfolded conformation. It should be noted that, as per density functional theory (DFT) calculations, which are described later, the proposed models appear to be suited for face-to-face interactions instead of edge-to-face ones. When rotation around the biphenyl C–C bond is slow on the ¹H NMR timescale, the population of the two conformers can be determined by integrating the ¹H signals of the methyl group (denoted by "Me" in

Figure 1) on ring Y. A 1,5-diethoxy-1,5-dioxopentan-3-yl (DDP) group^[22] was introduced at the *N*-position of the pyrrolidine ring for solubility reasons. Various substituents were embedded in the model system in order to elucidate the substituent effects: **1a–1f** contain a benzene ring (labelled ring Z), which is substituted with different functional groups at the *para* position (**1a**: -NMe₂, **1b**: -OMe, **1c**: -H, **1d**: -Cl, **1e**: -CN, **1f**: -NO₂), while **1g** contains a cyclohexyl group and **1h** contains a methyl group.

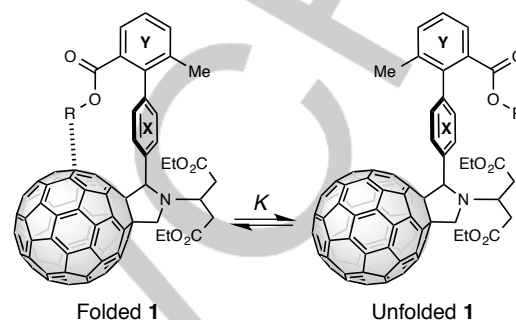
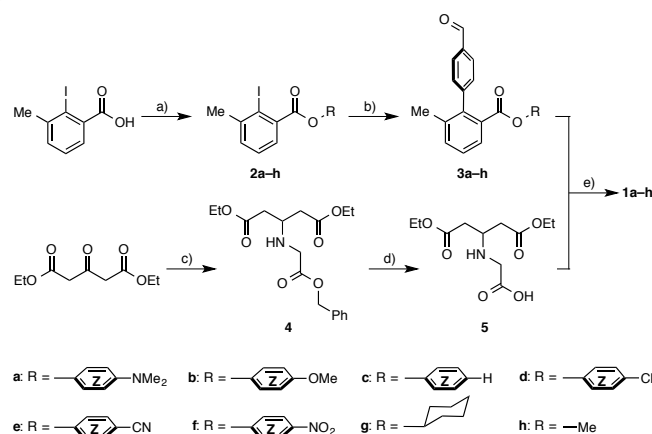


Figure 1. Fullerene-based molecular torsion balances (**1a–1h**) designed to study noncovalent interactions at fullerene surface.

The process for synthesizing the molecular torsion balances, **1a–1h**, is shown in Scheme 1. In short, the esterification of 2-iodo-3-methylbenzoic acid with the corresponding phenol or alcohol derivatives affords iodoarenes **2a–2h**. Next, Suzuki coupling with 4-formylboronic acid in the presence of PdCl₂(PPh₃)₂ and Na₂CO₃ yields aldehydes **3a–3h**. Meanwhile, the reductive amination of diethyl 1,3-acetonedicarboxylate with glycine benzyl ester hydrochloride in the presence of NaBH₃CN yields **4**, and the subsequent deprotection of the benzyl group results in glycine derivative **5**. Finally, the Prato reaction^[23] of C₆₀ with **3a–3h** and **5** in toluene affords **1a–1h** in yields of 23–44%. The characterization of **1a–1h** was performed using matrix-assisted laser desorption/ionization-time of flight mass spectrometry and absorption spectroscopy^[23] as well as by NMR spectral analyses.



Scheme 1. Synthesis of **1a–1h**. (a) R-OH, *N,N*-dimethyl-4-aminopyridine, *N,N*-dicyclohexylcarbodiimide, CH₂Cl₂. (b) 4-Formylboronic acid, PdCl₂(PPh₃)₂, Na₂CO₃, THF, H₂O, 80 °C. (c) Glycine benzyl ester hydrochloride, NaBH₃CN, MeOH. (d) Pd/C, EtOAc, MeOH, H₂. (e) C₆₀, toluene, 110 °C.

RESEARCH ARTICLE

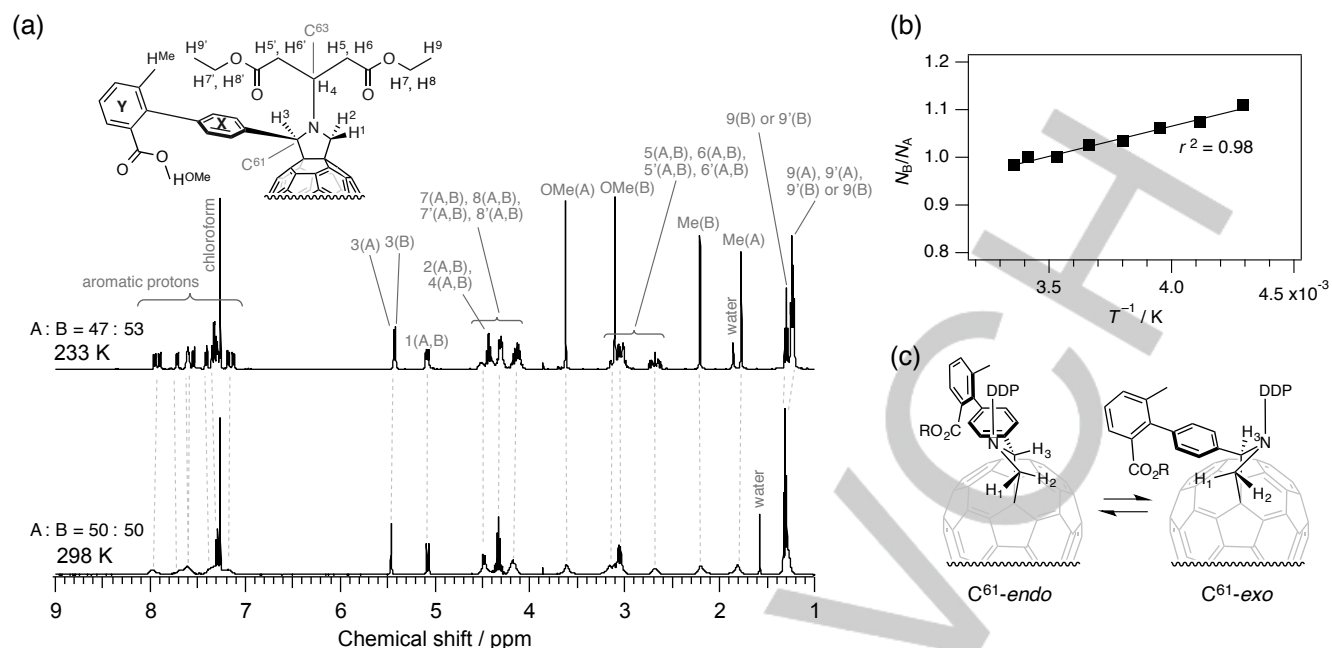


Figure 2. (a) 400 MHz ^1H NMR spectra of **1h** in CDCl_3 at 233 K and 298 K. Partial structure of **1h** as well as labelling system used are shown. Same labelling system was used for **1a–1g** throughout the manuscript, except for H^{OMe} . (b) Plot of N_B/N_A as a function of T^{-1} in CDCl_3 . (c) Schematic representation of possible nitrogen inversion of pyrrolidine ring of folded **1**.

NMR spectroscopic characterization and conformational analysis

Figure 2a shows the ^1H NMR spectra of **1h** in CDCl_3 at 298 K and 233 K as a typical example of the synthesized torsion balance systems. At 298 K, several signals appeared as broad resonances, and these signals became sharper with a decrease in the temperature. Notably, two sets of resonances for the methyl ($\text{H}^{\text{Me(A)}}$ and $\text{H}^{\text{Me(B)}}$) and methoxy ($\text{H}^{\text{OMe(A)}}$ and $\text{H}^{\text{OMe(B)}}$) protons on ring **Y** as well as two sets for the CH proton on the pyrrolidine ring ($\text{H}^{3(\text{A})}$ and $\text{H}^{3(\text{B})}$) were observed clearly in the spectra; this indicated the presence of two conformers, conformer-A and conformer-B. The relative integral ratio of conformer-A to conformer-B was 47:53 at 233 K. The large differences in the chemical shifts between $\text{H}^{\text{Me(A)}}$ and $\text{H}^{\text{Me(B)}}$ ($\Delta\delta = 0.44$ ppm at 233 K) as well as those between $\text{H}^{\text{OMe(A)}}$ and $\text{H}^{\text{OMe(B)}}$ ($\Delta\delta = 0.52$ ppm at 233 K) suggest that the methyl and methoxy groups on ring **Y** are located in significantly different environments in the two conformers. The two sets of the resonances ($\text{H}^{\text{Me(A)}}$ and $\text{H}^{\text{Me(B)}}$, and $\text{H}^{\text{OMe(A)}}$ and $\text{H}^{\text{OMe(B)}}$) do not coalesce in the 233–298 K range.^[24] In the rotating frame Overhauser enhancement spectroscopy (ROESY) spectrum of **1h** at 233 K, negative cross-peaks were observed between $\text{H}^{\text{Me(A)}}$ and $\text{H}^{\text{Me(B)}}$ as well as between $\text{H}^{\text{OMe(A)}}$ and $\text{H}^{\text{OMe(B)}}$, indicating that a chemical exchange had occurred between conformer-A and conformer-B over the NMR timescale. The relative populations of conformer-A and conformer-B (i.e., N_A and N_B , respectively; $N_A + N_B = 1$) were then determined by the integration of the Lorenz-fitted ^1H NMR signals of $\text{H}^{\text{Me(A)}}$ and $\text{H}^{\text{Me(B)}}$ at different temperatures. As shown in Figure 2b, N_B/N_A of **1h** was linearly dependent on T^{-1} in the range of 233–298 K ($r^2 = 0.98$).

Meanwhile, the four sets of triplets (three of which overlapped with each other) in the ^1H NMR spectrum of **1h** at 233 K could be assigned to the methyl protons of the ethoxy moieties, labeled H^9 and $\text{H}^{9'}$, indicating that the two ester units of the DDP group are

not equivalent and that the rotation around the $\text{N}-\text{C}^{63}$ bond is slower than the NMR timescale, owing to steric congestion.

As for the pyrrolidine ring of **1h**, the resonances of H^3 were observed as two singlets, at 5.46 ppm ($\text{H}^{3(\text{A})}$) and 5.45 ppm ($\text{H}^{3(\text{B})}$), at 233 K. Because the relative integral ratio of $\text{H}^{3(\text{A})}$ to $\text{H}^{3(\text{B})}$ was similar to that of $\text{H}^{\text{Me(A)}}$ to $\text{H}^{\text{Me(B)}}$, it is reasonable to conclude that the splitting of the resonances of H^3 into two at 233 K is attributable to the conformational isomerism between conformer-A and conformer-B. The two singlets of the H^3 resonances merged together as the temperature was increased and appeared as one singlet at 283–298 K.

The resonance of methylene proton H^2 could be distinguished from that of the other methylene proton, H^1 , based on the ROESY spectrum of **1h** at 233 K, wherein a positive cross-peak, that is, an ROE correlation, was observed between H^3 and H^2 . On the other hand, there was no correlation between H^3 and H^1 . The resonance of H^1 also appeared as two doublets, at 5.12 ppm ($^2J = 8.7$ Hz) and 5.11 ppm ($^2J = 8.7$ Hz), at 233 K. Further, these two doublets merged as the temperature was increased, appearing as a doublet ($^2J = 8.7$ Hz) at 283–298 K. Similar trends were also observed for the resonance of H^2 , though, in this case, the signals overlapped with the other proton signals (at 233 K, the resonance of H^2 appeared as a triplet because of overlapping with the other resonances).

Notably, the chemical shifts for H^1 and H^2 were markedly different in the range of 233–298 K ($\Delta\delta = 0.60$ – 0.64 ppm) regardless of the temperature, indicating that H^1 and H^2 were positioned in very different environments. In addition, the pyrrolidine protons would exhibit four sets of resonances if the nitrogen inversion of the pyrrolidine ring were to yield two observable conformers (see Figure 2c),^[25] because both conformer-A and conformer-B would split into two. However, this was not the case. Therefore, we surmised that the relative difference in the energies of one pyrrolidine conformer and the

RESEARCH ARTICLE

other nitrogen-inverted conformer is large enough such that only one side of the pyrrolidine conformers is responsible for the observed NMR resonances. This conclusion is further supported by the results of theoretical calculations, as described later. Thus, it can be concluded that the conformational isomerism between conformer-A and conformer-B comes from the restricted rotation around the biphenyl C–C bond between rings **X** and **Y**.

To gain further insights into the conformational behaviors, DFT calculations were performed at the M06-2X^[26]/6-31G(d)^[27] basis sets. The effects of chloroform as the solvent were

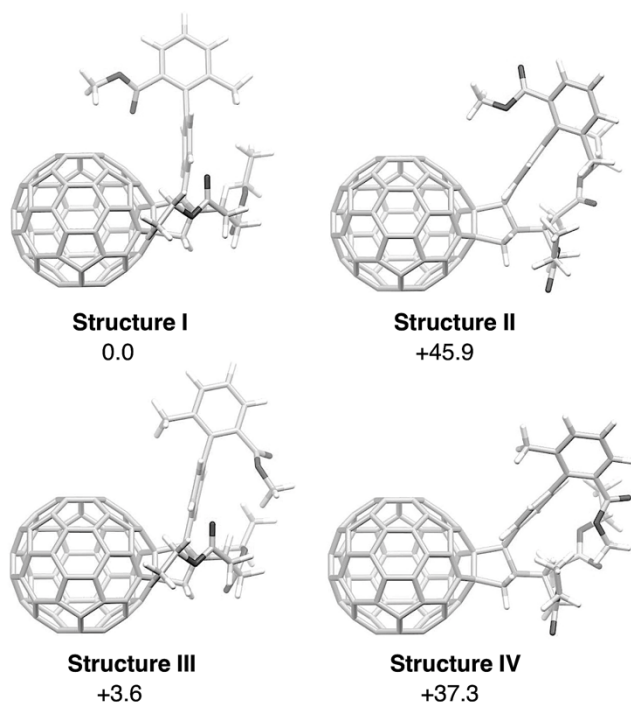


Figure 3. Optimized structures and relative energies (in kJ mol^{-1}) of four possible conformers (structures I, II, III, and IV) of **1h** determined using M06-2X^[26]/6-31G(d)^[27] level of theory. Effects of chloroform as solvent were introduced through self-consistent reaction field theory calculations performed using IEFPCM method.^[28]

introduced based on self-consistent reaction field theory calculations performed using the IEFPCM method.^[28] Figure 3 shows four possible conformers of **1h** as representative molecular torsion balances as well as their relative energies.

Structures I and II correspond to the folded conformers while structures III and IV correspond to the unfolded conformers with respect to the restricted rotation around the C–C bond between rings **X** and **Y**. In addition, structures I and III exhibit the C₆₁-endo form whereas structures II and IV exhibit the C⁶¹-exo form with respect to the nitrogen atom of the pyrrolidine ring. The results indicated that the C⁶¹-exo conformers are 37–46 kJ mol^{-1} less stable than the C⁶¹-endo conformers. Thus, it is reasonable to conclude that the contribution of the C⁶¹-exo conformers to the ¹H NMR spectra is negligible and that the C⁶¹-endo forms are the dominant ones. In addition, structures I and III of **1h** have similar stabilities. These results are in good agreement with those of ¹H NMR spectral studies, which showed that the differences in the free energies of **1h** are small. The separation between the methyl proton and the nearest carbon of the fullerene cage in structure I was calculated to be 2.8 Å, which is similar to the sum of the van

der Waals radii of the relevant nuclei (~2.9 Å). In a related work, Nishio et al. reported that the C–H⋯fullerene distance was determined to be 2.9 Å or lower (as low as 2.5 Å), as per a survey by the Cambridge Crystallographic Database.^[29] The DFT calculations also suggested that the optimized structure of the folded conformation of **1a** has the face-to-face configuration, as shown in Figure 4. The smallest C⋯C distance between ring **Z** and the fullerene surface was calculated to be 3.0 Å. The nitrogen atom of the *N,N*-dimethylamino group on ring **Z** was also located close to the fullerene carbon atom, and the interatomic distance was 3.2 Å. These results suggest that the rigid framework of the proposed model system ensures intramolecular face-to-face arene–fullerene interactions, in keeping with expectations.

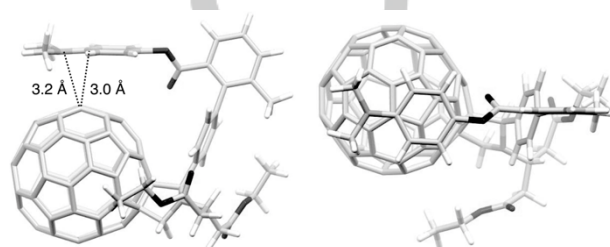


Figure 4. Two orthogonal views of optimized structure of folded conformation of **1a** determined using M06-2X^[26]/6-31G(d)^[27] level of theory. Effects of chloroform as solvent were introduced through self-consistent reaction field theory calculations performed using IEFPCM method.^[28]

The ¹H NMR chemical shifts were calculated for structures I and III at the GIAO^[30]-B3LYP^[31]/6-31G(d) level of theory using the M06-2X^[26]/6-31G(d)^[27] optimized geometries.^[32] We focused on the H^{Me} protons as the indicators of the conformers, because the methyl group is the one least affected by the local ring currents of the C₆₀ core^[33] and the flexible DDP moieties. The calculated average ¹H chemical shift of the H^{Me} protons in structure I appears at a lower magnetic field (2.06 ppm) than that in structure III (1.91 ppm). Therefore, it is suggested that conformer-A and conformer-B are the unfolded and folded conformers, respectively. Based on this assignment, the folding free energies (ΔG_{fold}) can be obtained from Equation (1).

$$\Delta G_{\text{fold}} = -RT \ln(N_B/N_A) \quad (1)$$

The ΔG_{fold} value of **1h** (0.06 kJ mol^{-1} in CDCl₃) is close to zero, indicating that the relative energies of conformer-A and conformer-B are almost identical. Thus, it is reasonable to conclude that, because of the negligibly weak interaction between R and the fullerene surface, conformer-A and conformer-B are almost isoenergetic in **1h** and that the very small ΔG_{fold} value may be attributable to the solvent effects and long-range polar interactions.

The ¹H NMR spectra of **1a–1h** at 233 K exhibited very similar ¹H chemical shifts and spin–spin coupling patterns for the protons common to **1a–1h**. This suggested similar conformational isomerism, that is, the existence of only two NMR-detectable conformers (conformer-A and conformer-B), in **1a–1h** (see Figure S111). Thus, we assigned the respective conformers-A and -B of **1a–1h** based on the similarities in the chemical shifts as well as the patterns in their ¹H NMR spectra. The folding free energy, ΔG_{fold} , values at 298 K in CDCl₃ and C₆D₆, obtained from Eq. 1, are listed in Table 1. The corresponding Hammett constants

RESEARCH ARTICLE

(σ_{para}),^[34] and experimental polarizability (α) values^[35,36] of the corresponding R-H molecules for **1a–1h** are also shown in the table. Finally, Figure 5 shows the relationship between the individual ΔG_{fold} values and the Hammett constant for the substituent R.

Table 1. Folding free energy (ΔG_{fold}) values of **1a–1h**; Hammett constant, σ_{p} , for substituents in ring **Z**; and polarizability (α) values of corresponding R-H molecules

Compd.	$\Delta G_{\text{fold}}^{[\text{a}]}$ in CDCl_3	$\Delta G_{\text{fold}}^{[\text{a}]}$ in C_6D_6	$\sigma_{\text{p}}^{[\text{b}]}$	α
1a (R = $\text{C}_6\text{H}_4\text{NMe}_2$)	-0.20	-0.46	-0.83	16.3 ^[f]
1b (R = $\text{C}_6\text{H}_4\text{OMe}$)	0.18	-0.07	-0.27	13.1 ^[f]
1c (R = C_6H_5)	0.78	0.71	0.00	10.4 ^[f]
1d (R = $\text{C}_6\text{H}_4\text{Cl}$)	0.43	- ^[d]	0.23	12.4 ^[f]
1e (R = $\text{C}_6\text{H}_4\text{CN}$)	1.14	1.68	0.66	12.6 ^[f]
1f (R = $\text{C}_6\text{H}_4\text{NO}_2$)	0.91	1.46	0.78	13 ^[f]
1g (R = cyclohexyl)	1.02 ^[c]	- ^[d]	N/A ^[e]	11.0 ^[f]
1h (R = methyl)	0.06	0.22	N/A ^[e]	2.6 ^[g]

[a] All data are average values in kJ mol^{-1} obtained from multiple measurements. Uncertainty is $\pm 0.12 \text{ kJ mol}^{-1}$. [b] Ref. 34. [c] Integral ratio of H^3 signals instead of those of H^{Me} were used for determining thermodynamic parameters because of overlapping of H^{Me} and proton signals of cyclohexyl group. [d] Data could not be obtained because solubility was too low. [e] Not applicable. [f] Values in \AA^3 ; Ref. 35. [g] Values in \AA^3 ; Ref. 36.

Substituent effects

It is worth noting that the ΔG_{fold} values varied with the choice of R in **1a–1h**. Based on the similarity of the structures of **1a–1h**, we propose that the noncovalent interactions between R and the fullerene surface are responsible for the differences in the ΔG_{fold} values. The observed positive ΔG_{fold} values indicate that the primary contributors are the Pauli repulsion terms, which direct the molecular torsion balances to the unfolded conformers, in the case of **1b–1g** in CDCl_3 . As shown in Figure 5, the ΔG_{fold} values were correlated not with the α values of the corresponding R-H molecules but with their σ_{p} values in the aromatic systems.

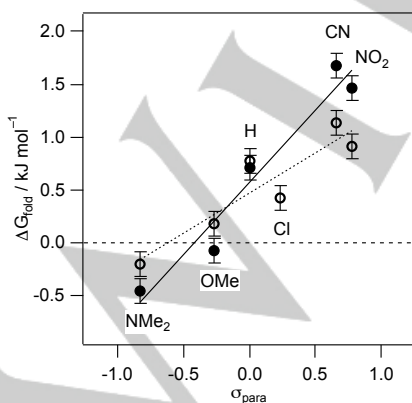


Figure 5. Experimental ΔG_{fold} values in CDCl_3 (open circles) and C_6D_6 (solid circles) plotted against Hammett constant σ_{para} of respective substituents in ring **Z**.

The high linearity of the correlation of ΔG_{fold} with σ_{p} in the aromatic systems both in CDCl_3 ($r^2 = 0.83$) and in C_6D_6 ($r^2 = 0.95$) can be explained based on electrostatic interactions. These interactions direct the molecular torsion balances to the folded conformers and are counterbalanced by the Pauli repulsion terms. The results also suggest that the noncovalent interactions between the arene moieties and the fullerene surface become more attraction-based as the π -electron density of R increases. This trend is in contrast to that observed in the case of the face-to-face arene–arene interactions, wherein electron-withdrawing substituents lead to the stabilization of the interactions while electron-donating substituents destabilize the interactions. The magnitude of the positive slope (0.76 kJ mol^{-1}) is smaller than those measured by Gung et al. ($-3.24 \text{ kJ mol}^{-1}$; $r^2 = 0.94$),^[19a] and Shimizu et al. ($-0.80 \text{ kJ mol}^{-1}$; $r^2 = 0.41$ for the phenanthrene system)^[19] for flat aromatic surfaces that face-to-face stack in CDCl_3 . Diederich et al. also observed a linear correlation between the association constants and the σ_{p} values in a bimolecular host–guest model system consisting of a Rebek-imide-type receptor; this correlation was indicative of the electrostatic effects of the substituent on the aromatic platform of the receptor with respect to the parallel-displaced face-to-face arene–arene interactions, as predicted by the Hunter–Sanders model.^[37] The opposite correlations of the folding energies with σ_{p} values between the arene–arene interactions and arene–fullerene interactions could be related to the unique electrostatic potentials and the strong electron-accepting ability of C_{60} . In the case of **1a**, ΔG_{fold} is negative, indicating that the attractive electrostatic interactions overcome the repulsive interactions to direct the folded conformer more preferably in CDCl_3 . The substituent effect is more pronounced in C_6D_6 than that in CDCl_3 . The fact that the substituent effect is stronger in the apolar solvent than in the polar one can be explained based on the solute–solvent interactions.^[18b,38] This is in keeping with the distinct contribution of the electrostatic interactions between the organic moieties and the fullerene surface. In fact, the ΔG_{fold} value of **1b** becomes negative when the solvent is changed from CDCl_3 to C_6D_6 . This trend contrasts with that observed for the complexation between C_{60} and calix[4]arene-linked bis-porphyrins reported by Boyd and coworkers. In their system, the binding constant and fullerene solubility were found to be inversely correlated, indicating that desolvation of the fullerene was a major factor determining the magnitude of the binding constant.^[5e] The ΔG_{fold} value is larger when ring **Z** is unsubstituted (i.e., **1c**) as compared with that for the chloro-substituted system, **1d**. This deviation from the correlation between ΔG_{fold} and σ_{p} could be due to the difference in the dispersion interactions and/or the absence of direct interactions between the substituent of the arene ring and the fullerene surface. In a related study, Wheeler and Houk showed that, in the case of the correlation between the computed gas-phase interaction energies and the Hammett constants for sandwich dimers of benzenes, there exists an outlier, namely, the unsubstituted benzene dimer.^[13f] They stated that this deviation was attributable to the dispersion interactions, which supposedly stabilize all types of substituted benzene dimers, in contrast to the case for the unsubstituted benzene dimer. In fact, the R-H for **1c** exhibits smaller polarizability values than those for **1a**, **1b**, **1d**, **1e**, and **1f**. The DFT-calculated folding free energies for **1a–1f** using the M06-2X^[26]/6-31G(d)^[27] level of theory and the IEFPCM method^[28] are essentially reproduce the experimental trends, as shown in Figure S120. This observation suggests that substituted

RESEARCH ARTICLE

arenes having negative and positive σ_p values favor folded and unfolded conformers, respectively, while unsubstituted arenes highly disfavor folded conformers. The large ΔG_{fold} value of **1g** can also be explained based on the low polarizability of the cyclohexyl moiety, which contributed to the dispersion term. It is likely that the possible edge-to-face aliphatic CH–fullerene interaction is overwhelmed by the repulsive terms. On the whole, the substituent effects observed in these experiments suggest that the electrostatic interactions have a significant influence on the arene–fullerene interactions.

Conclusion

In summary, we attempted to quantify the noncovalent interactions between organic moieties and the fullerene surface by examining the conformational equilibrium of newly designed fullerene-based molecular torsion balances. With this aim in mind, we successfully synthesized the corresponding model system through the Prato reactions of C_{60} with the corresponding aldehydes and characterized the fullerene-based torsion balances. We found that two conformers corresponding to the folded and unfolded states are observable based on their ^1H NMR spectra, allowing us to determine the thermodynamic parameters corresponding to the noncovalent interactions occurring on the fullerene surface. The results also showed clearly that the interactions are very weak but measurable. In addition, the electrostatic interactions contribute to the overall interactions between the arene moieties and the fullerene surface, while dispersion interactions play an important role in the case of the folding conformer. The difference in the free energies was 1.34 kJ mol $^{-1}$ in CDCl_3 and 2.14 kJ mol $^{-1}$ in C_6D_6 . The results presented herein highlight the utility of unimolecular balance systems for the experimental quantification of weak interactions on the fullerene surface. The limitations of the presented model system, however, is the difficulty in designing double-mutant cycles to extract the energetics of a selected interaction. Nevertheless, this study provides valuable data not only for computational chemists who aim to study noncovalent interactions on curved nanocarbons such as fullerenes and carbon nanotubes but also for medicinal chemists exploring nanocarbon-based pharmaceutical agents. Future efforts will be devoted to elucidating other intermolecular interactions such as heteroarene–fullerene interactions and anion–fullerene interactions by tuning the design of the fullerene-based molecular balances.

Supporting Information: Synthetic procedures, HPLC profiles, mass spectra, absorption spectra, NMR studies, and NMR spectra of new compounds (PDF)

Acknowledgements

The work was supported by the Asahi Glass Foundation. We thank Prof. Dr. Yoko Yamakoshi and Ms. Liosi Korinne (ETH Zürich) for valuable comments on the synthesis of glycine derivatives. We also thank Mr. Y. Fujiwara for his assistance with the experiments.

Keywords: fullerenes • conformational analysis • pi interactions • electrostatic interactions • London dispersion force

- [1] *Supramolecular Chemistry of Fullerenes and Carbon Nanotubes*, eds. N. Martin and J.-F. Nierengarten, Wiley-VCH, Weinheim, 2012.
- [2] a) S. Chakrabarti, K. Ruud, *J. Phys. Chem. A* **2009**, *113*, 5485-5488; b) M. d. C. Gimenez-Lopez, M. T. Räisänen, T. W. Chamberlain, U. Weber, M. Lebedeva, G. A. Rance, G. A. D. Briggs, D. Pettifor, V. Burlakov, M. Buck, A. N. Khlobystov, *Langmuir* **2011**, *27*, 10977-10985; c) K. Campbell, B. Gurum, B. G. Sumpter, Y. S. Thio, D. G. Bucknall, *J. Phys. Chem. B* **2011**, *115*, 8989-8995; d) M. P. Evstigneev, A. S. Buchelnikov, D. P. Voronin, Y. V. Rubin, L. F. Belous, Y. I. Prylutskiy, U. Ritter, *ChemPhysChem* **2013**, *14*, 568-578; e) K. R. Graham, C. Cabanetos, J. P. Jahnke, M. N. Idso, A. E. Labban, G. O. N. Ndjawa, T. Heumueller, K. Vandewal, A. Salleo, B. F. Chmelka, A. Amassian, P. M. Beaujuge, M. D. McGehee, *J. Am. Chem. Soc.* **2014**, *136*, 9608-9618; f) Y.-Y. Lai, M.-H. Liao, Y.-T. Chen, F.-Y. Cao, C.-S. Hsu, Y.-J. Cheng, *ACS Appl. Mater. Interfaces* **2014**, *6*, 20102-20109; g) S. Sweetnam, K. Vandewal, E. Cho, C. Risko, V. Coropceanu, A. Salleo, J.-L. Bredas, M. D. McGehee, *Chem. Mater.* **2016**, *28*, 1446-1452; h) W. Tress, B. Beyer, N. A. Astani, F. Gao, S. Meloni, U. Rothlisberger, *J. Phys. Chem. Lett.* **2016**, *7*, 3936-3944; i) J. Li, X. Zhu, T. Yuan, J. Shen, J. Liu, J. Zhang, G. Tu, *ACS Appl. Mater. Interfaces* **2017**, *9*, 6615-6623.
- [3] a) J. López-Andarias, A. Frontera, S. Matile, *J. Am. Chem. Soc.* **2017**, *139*, 13296-13299; b) J. López-Andarias, A. Bauzá, N. Sakai, A. Frontera, S. Matile, *Angew. Chem.* **2018**, *130*, 11049-11053; *Angew. Chem. Int. Ed.* **2018**, *57*, 10883-10887; c) X. Zhang, L. Liu, J. López-Andarias, C. Wang, N. Sakai, S. Matile, *Helv. Chim. Acta* **2018**, *101*, e1700288.
- [4] a) P. D. W. Boyd, C. A. Reed, *Acc. Chem. Res.* **2005**, *38*, 235-242; b) K. Tashiro, T. Aida, *Chem. Soc. Rev.* **2007**, *36*, 189-197; c) S. Selmani, D. J. Schipper, *Chem. Eur. J.* **2019**, *25*, 6673-6692.
- [5] a) K. Tashiro, T. Aida, J.-Y. Zheng, K. Kinbara, K. Saigo, S. Sakamoto, K. Yamaguchi, *J. Am. Chem. Soc.* **1999**, *121*, 9477-9478; b) D. Sun, F. S. Tham, C. A. Reed, L. Chaker, M. Burgess, P. D. W. Boyd, *J. Am. Chem. Soc.* **2000**, *122*, 10704-10705; c) D. Sun, F. S. Tham, C. A. Reed, L. Chaker, P. D. W. Boyd, *J. Am. Chem. Soc.* **2002**, *124*, 6604-6612; d) Y. Shoji, K. Tashiro, T. Aida, *J. Am. Chem. Soc.* **2006**, *128*, 10690-10691; e) A. Hosseini, S. Taylor, G. Accorsi, N. Armaroli, C. A. Reed, P. D. W. Boyd, *J. Am. Chem. Soc.* **2006**, *128*, 15903-15913; f) M. Yanagisawa, K. Tashiro, M. Yamasaki, T. Aida, *J. Am. Chem. Soc.* **2007**, *129*, 11912-11913; g) L. H. Tong, J.-L. Wietor, W. Clegg, P. R. Raithby, S. I. Pascu, J. K. M. Sanders, *Chem. Eur. J.* **2008**, *14*, 3035-3044; h) Y. Shoji, K. Tashiro, T. Aida, *J. Am. Chem. Soc.* **2010**, *132*, 5928-5929; i) J. Song, N. Aratani, H. Shinokubo, A. Osuka, *J. Am. Chem. Soc.* **2010**, *132*, 16356-16357; j) G. Gil-Ramírez, S. D. Karlen, A. Shundo, K. Porfyrakis, Y. Ito, G. A. D. Briggs, J. J. L. Morton, H. L. Anderson, *Org. Lett.* **2010**, *12*, 3544-3547; k) H. Nobukuni, Y. Shimazaki, H. Uno, Y. Naruta, K. Ohkubo, T. Kojima, S. Fukuzumi, S. Seki, H. Sakai, T. Hasobe, F. Tani, *Chem. Eur. J.* **2010**, *16*, 11611-11623; l) L. P. Hernández-Eguía, E. C. Escudero-Adán, J. R. Pinzón, L. Echegoyen, P. Ballester, *J. Org. Chem.* **2011**, *76*, 3258-3265; m) X. Fang, Y.-Z. Zhu, J.-Y. Zheng, *J. Org. Chem.* **2014**, *79*, 1184-1191; n) C. Yu, H. Long, Y. Jin, W. Zhang, *Org. Lett.* **2016**, *18*, 2946-2949; o) P. Mondal, S. P. Rath, *Chem. Asian J.* **2017**, *12*, 1824-1835.
- [6] a) T. Kawase, K. Tanaka, N. Fujiwara, H. R. Darabi, M. Oda, *Angew. Chem.* **2003**, *115*, 1662-1666; *Angew. Chem. Int. Ed.* **2003**, *42*, 1624-1628; b) T. Kawase, K. Tanaka, N. Shiono, Y. Seirai, M. Oda, *Angew. Chem.* **2004**, *116*, 1754-1756; *Angew. Chem. Int. Ed.* **2004**, *43*, 1722-1724; c) T. Kawase, N. Fujiwara, M. Tsutumi, M. Oda, Y. Maeda, T. Wakahara, T. Akasaka, *Angew. Chem.* **2004**, *116*, 5170-5172; *Angew. Chem. Int. Ed.* **2004**, *43*, 5060-5062; d) A. Sygula, F. R. Fronczek, R. Sygula, P. W. Rabideau, M. M. Olmstead, *J. Am. Chem. Soc.* **2007**, *129*, 3842-3843; e) C. Muck-Lichtenfeld, S. Grimme, L. Kobryn, A. Sygula, *Phys. Chem. Chem. Phys.* **2010**, *12*, 7091-7097; f) T. Iwamoto, Y. Watanabe, T. Sadahiro, T. Haino, S. Yamago, *Angew. Chem.* **2011**, *123*, 8492-8494; *Angew. Chem. Int. Ed.* **2011**, *50*, 8342-8344; g) H. Isobe, S. Hitosugi, T. Yamasaki, R. Iizuka, *Chem. Sci.* **2013**, *4*, 1293-1297; h) S. Hitosugi, R. Iizuka, T. Yamasaki, Y. Murata, H. Isobe, *Org. Lett.* **2013**,

RESEARCH ARTICLE

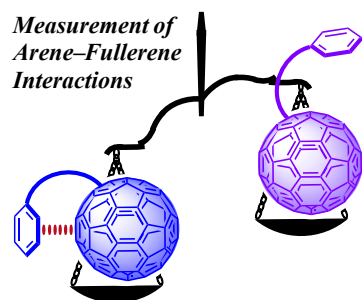
- 15, 3199-3201; i) V. H. Le, M. Yanney, M. McGuire, A. Sygula, E. A. Lewis, *J. Phys. Chem. B* **2014**, *118*, 11956-11964; j) H. Ueno, T. Nishihara, Y. Segawa, K. Itami, *Angew. Chem.* **2015**, *127*, 3778-3782; *Angew. Chem. Int. Ed.* **2015**, *54*, 3707-3711; k) K-S. Liu, M.-J. Li, C.-C. Lai, S.-H. Chiu, *Chem. Eur. J.* **2016**, *22*, 17468-17476; l) T. Matsuno, Y. Nakai, S. Sato, Y. Maniwa, H. Isobe, *Nat. Commun.* **2018**, *9*:1907; doi: 10.1038/s41467-018-04325-2; m) M. Takeda, S. Hiroto, H. Yokoi, S. Lee, D. Kim, H. Shinokubo, *J. Am. Chem. Soc.* **2018**, *140*, 6336-6342; n) Y. Yamamoto, E. Tsurumaki, K. Wakamatsu, S. Toyota, *Angew. Chem.* **2018**, *130*, 8331-8334; *Angew. Chem. Int. Ed.* **2018**, *57*, 8199-8202; o) Z. Sun, T. Mio, T. Okada, T. Matsuno, S. Sato, H. Kono, H. Isobe, *Angew. Chem.* **2019**, *131*, 2062-2066; *Angew. Chem. Int. Ed.* **2019**, *58*, 2040-2044.
- [7] a) Y. Inokuma, T. Arai, M. Fujita, *Nat. Chem.* **2010**, *2*, 780-783; b) C. García-Simón, M. García-Borrás, L. Gómez, T. Parella, S. Osuna, J. Juanhuix, I. Imaz, D. Maspocho, M. Costas, X. Ribas, *Nat. Commun.* **2014**, *5*:557; doi: 10.1038/ncomms6557; c) T. K. Ronson, A. B. League, L. Gagliardi, C. J. Cramer, J. R. Nitschke, *J. Am. Chem. Soc.* **2014**, *136*, 15615-15624; d) D. M. Wood, W. Meng, T. K. Ronson, A. R. Stefankiewicz, J. K. M. Sanders, J. R. Nitschke, *Angew. Chem.* **2015**, *127*, 4060-4064; *Angew. Chem. Int. Ed.* **2015**, *54*, 3988-3992; e) T. K. Ronson, B. S. Pilgrim, J. R. Nitschke, *J. Am. Chem. Soc.* **2016**, *138*, 10417-10420; f) D. Rackauskaite, R. Gegevičius, Y. Matsuo, K. Wärnmark, E. Orentas, *Angew. Chem.* **2016**, *128*, 216-220; *Angew. Chem. Int. Ed.* **2016**, *55*, 208-212; g) W. Brenner, T. K. Ronson, J. R. Nitschke, *J. Am. Chem. Soc.* **2017**, *139*, 75-78; h) T. K. Ronson, W. Meng, J. R. Nitschke, *J. Am. Chem. Soc.* **2017**, *139*, 9698-9707; i) F. J. Rizzuto, D. M. Wood, T. K. Ronson, J. R. Nitschke, *J. Am. Chem. Soc.* **2017**, *139*, 11008-11011; j) A. J. Musser, P. P. Neelakandan, J. M. Richter, H. Mori, R. H. Friend, J. R. Nitschke, *J. Am. Chem. Soc.* **2017**, *139*, 12050-12059; k) N. Struch, C. Bannwarth, T. K. Ronson, Y. Lorenz, B. Mienert, N. Wagner, M. Engeser, E. Bill, R. Puttreddy, K. Rissanen, J. Beck, S. Grimme, J. R. Nitschke, A. Lützen, *Angew. Chem.* **2017**, *129*, 5012-5017; *Angew. Chem. Int. Ed.* **2017**, *56*, 4930-4935; l) F. J. Rizzuto, J. R. Nitschke, *Nat. Chem.* **2017**, *9*, 903-908.
- [8] a) S. Bhattacharya, A. K. Bauri, S. Chattopadhyay, M. Banerjee, *J. Phys. Chem. B* **2005**, *109*, 7182-7187; b) R. P. Kopreski, J. B. Briggs, W. Lin, M. Jazdzzyk, G. P. Miller, *J. Org. Chem.* **2012**, *77*, 1308-1315; c) A. Tkatchenko, D. Alfe, K. S. Kim, *J. Chem. Theory Comput.* **2012**, *8*, 4317-4322; d) M.-M. Li, Y.-B. Wang, Y. Zhang, W. Wang, *J. Phys. Chem. A* **2016**, *120*, 5766-5772; e) Y. Zhang, W. Wang, Y.-B. Wang, *Comput. Theor. Chem.* **2017**, *1122*, 34-39; f) C. J. Chancellor, F. L. Bowles, J. U. Franco, D. M. Pham, M. Rivera, E. A. Sarina, K. B. Ghiassi, A. L. Balch, M. M. Olmstead, *J. Phys. Chem. A* **2018**, *122*, 9626-9636; g) H. Mönig, S. Amirjalayer, A. Timmer, Z. Hu, L. Liu, O. D. Arado, M. Cnudde, C. A. Strasser, W. Ji, M. Rohlfing, H. Fuchs, *Nat. Nanotechnol.* **2018**, *13*, 371-375.
- [9] Nierengarten et al. performed SAPT calculations on metalloporphyrin-methano[60]fullerene cup-and-ball complexes and deconvolved the total binding energy into electrostatic, exchange, induction, and dispersion energy components, in addition to the electrochemical and titration studies: L. Moreira, J. Calbo, B. M. Illescas, J. Aragó, I. Nierengarten, B. Delavaux-Nicot, E. Ortí, N. Martín, J.-F. Nierengarten, *Angew. Chem.* **2015**, *127*, 1271-1276; *Angew. Chem. Int. Ed.* **2015**, *54*, 1255-1260.
- [10] B. Jeziorski, R. Moszynski, K. Szalewicz, *Chem. Rev.* **1994**, *94*, 1887-1930.
- [11] *Noncovalent Forces. Challenges and Advances in Computational Chemistry and Physics*, 19, ed. S. Scheiner, Springer, Cham, **2015**.
- [12] *Aromatic Interactions: Frontiers in Knowledge and Application*, eds. D. W. Johnson and J. Fraser Hof, The Royal Society of Chemistry, Cambridge, **2017**.
- [13] a) L. F. Newcomb, S. H. Gellman, *J. Am. Chem. Soc.* **1994**, *116*, 4993-4994; b) F. Cozzi, J. S. Siegel, *Pure Appl. Chem.* **1995**, *67*, 683-689; c) R. R. Gardner, L. A. Christianson, S. H. Gellman, *J. Am. Chem. Soc.* **1997**, *119*, 5041-5042; d) K. Nakamura, K. N. Houk, *Org. Lett.* **1999**, *1*, 2049-2051; e) M. O. Sinnokrot, C. D. Sherrill, *J. Phys. Chem. A* **2003**, *107*, 8377-8379; f) S. E. Wheeler, K. N. Houk, *J. Am. Chem. Soc.* **2008**, *130*, 10854-10855; g) A. L. Ringer, C. D. Sherrill, *J. Am. Chem. Soc.* **2009**, *131*, 4574-4575; h) S. E. Wheeler, A. J. McNeil, P. Müller, T. M. Swager, K. N. Houk, *J. Am. Chem. Soc.* **2010**, *132*, 3304-3311; i) M. Watt, L. K. E. Hardebeck, C. C. Kirkpatrick, M. Lewis, *J. Am. Chem. Soc.* **2011**, *133*, 3854-3862; j) S. E. Wheeler, *J. Am. Chem. Soc.* **2011**, *133*, 10262-10274; k) C. D. Sherrill, *Acc. Chem. Res.* **2013**, *46*, 1020-1028.
- [14] a) C. A. Hunter, J. K. M. Sanders, *J. Am. Chem. Soc.* **1990**, *112*, 5525-5534; b) C. A. Hunter, K. R. Lawson, J. Perkins, C. J. Urch, *J. Chem. Soc., Perkin Trans. 2*, **2001**, *5*, 651-669.
- [15] a) T. H. Webb, C. S. Wilcox, *J. Org. Chem.* **1990**, *55*, 363-365; b) S. Paliwal, S. Geib, C. S. Wilcox, *J. Am. Chem. Soc.* **1994**, *116*, 4497-4498; c) E.-i. Kim, S. Paliwal, C. S. Wilcox, *J. Am. Chem. Soc.* **1998**, *120*, 11192-11193.
- [16] B. Bhayana, *J. Org. Chem.* **2013**, *78*, 6758-6762.
- [17] For recent reviews, see: a) I. K. Mati, S. L. Cockroft, *Chem. Soc. Rev.* **2010**, *39*, 4195-4205; b) M. A. Strauss, H. A. Wegner, *Eur. J. Org. Chem.* **2019**, 295-302; c) A. E. Aliev, W. B. Motherwell, *Chem. Eur. J.* **2019**, *25*, 10516-10530.
- [18] For examples of Wilcox torsion balances, see: a) F. Hof, D. M. Scofield, W. B. Schweizer, F. Diederich, *Angew. Chem.* **2004**, *116*, 5166-5169; *Angew. Chem. Int. Ed.* **2004**, *43*, 5056-5059; b) S. L. Cockroft, C. A. Hunter, *Chem. Commun.* **2006**, 3806-3808; c) B. Bhayana, C. S. Wilcox, *Angew. Chem.* **2007**, *119*, 6957-6960; *Angew. Chem. Int. Ed.* **2007**, *46*, 6833-6836; d) F. R. Fischer, W. B. Schweizer, F. Diederich, *Angew. Chem.* **2007**, *119*, 8418-8421; *Angew. Chem. Int. Ed.* **2007**, *46*, 8270-8273; e) F. R. Fischer, W. B. Schweizer, F. Diederich, *Chem. Commun.* **2008**, 4031-4033; f) F. R. Fischer, P. A. Wood, F. H. Allen, F. Diederich, *Proc. Natl. Acad. Sci. USA* **2008**, *105*, 17290-17294; g) W. R. Carroll, P. Pellechia, K. D. Shimizu, *Org. Lett.* **2008**, *10*, 3547-3550; h) S. L. Cockroft, C. A. Hunter, *Chem. Commun.* **2009**, 3961-3963; i) L. Yang, C. Adam, G. S. Nichol, S. L. Cockroft, *Nat. Chem.* **2013**, *5*, 1006-1010; j) B. Bhayana, *J. Org. Chem.* **2013**, *78*, 6758-6762; k) H. Gardarsson, W. B. Schweizer, N. Trapp, F. Diederich, *Chem. Eur. J.* **2014**, *20*, 4608-4616; l) C. Adam, L. Yang, S. L. Cockroft, *Angew. Chem.* **2015**, *127*, 1180-1183; *Angew. Chem. Int. Ed.* **2015**, *54*, 1164-1167; i) L. Yang, C. Adam, S. L. Cockroft, *J. Am. Chem. Soc.* **2015**, *137*, 10084-10087; j) X. Ling, C. S. Wilcox, *Chem. Eur. J.* **2019**, *25*, 14010-14014.
- [19] For examples of molecular balances other than Wilcox torsion balances, see: a) b) W. B. Motherwell, J. Moïse, A. E. Aliev, M. Nic, S. J. Coles, P. N. Horton, M. B. Hursthouse, G. Chessari, C. A. Hunter, J. G. Vinter, *Angew. Chem.* **2007**, *119*, 7969-7972; *Angew. Chem. Int. Ed.* **2007**, *46*, 7823-7826; c) W. R. Carroll, P. Pellechia, K. D. Shimizu, *Org. Lett.* **2008**, *10*, 3547-3550; d) Y. S. Chong, W. R. Carroll, W. G. Burns, M. D. Smith, K. D. Shimizu, *Chem. Eur. J.* **2009**, *15*, 9117-9126; e) W. R. Carroll, C. Zhao, M. D. Smith, P. J. Pellechia, K. D. Shimizu, *Org. Lett.* **2011**, *13*, 4320-4323; f) J. L. Xia, S. H. Liu, F. Cozzi, M. Mancinelli, A. Mazzanti, *Chem. Eur. J.* **2012**, *18*, 3611-3620; g) K. B. Muchowska, C. Adam, I. K. Mati, S. L. Cockroft, *J. Am. Chem. Soc.* **2013**, *135*, 9976-9979; h) I. K. Mati, C. Adam, S. L. Cockroft, *Chem. Sci.* **2013**, *4*, 3965-3972; i) J. Hwang, P. Li, W. R. Carroll, M. D. Smith, P. J. Pellechia, K. D. Shimizu, *J. Am. Chem. Soc.* **2014**, *136*, 14060-14067; j) A. E. Aliev, J. R. T. Arendorf, I. Pavlakos, R. B. Moreno, M. J. Porter, H. S. Rzepa, W. B. Motherwell, *Angew. Chem.* **2015**, *127*, 561-565; *Angew. Chem. Int. Ed.* **2015**, *54*, 551-555; k) I. Pavlakos, T. Arif, A. E. Ariev, W. B. Motherwell, G. J. Tizzard, S. J. Coles, *Angew. Chem.* **2015**, *127*, 8287-8292; *Angew. Chem. Int. Ed.* **2015**, *54*, 8169-8174; l) J. M. Maier, P. Li, J. Hwang, M. D. Smith, K. D. Shimizu, *J. Am. Chem. Soc.* **2015**, *137*, 8014-8017; m) S. Yamada, N. Yamamoto, E. Takamori, *J. Org. Chem.* **2016**, *81*, 11819-11830; n) J. Luccarelli, I. M. Jones, S. Thompson, A. D. Hamilton, *Org. Biomol. Chem.* **2017**, *15*, 9156-9163; o) W. B. Motherwell, R. B. Moreno, I. Pavlakos, J. R. T. Arendorf, T. Arif, G. J. Tizzard, S. J. Coles, A. E. Aliev, *Angew. Chem.* **2018**, *130*, 1207-1212; *Angew. Chem. Int. Ed.* **2018**, *57*, 1193-1198; p) J. M. Maier, P. Li, J. S. Ritchey, C. J. Yehl, K. D. Shimizu, *Chem. Commun.* **2018**, *54*, 8502-8505; q) J. Hwang, P. Li, E. C. Vik, I. Karki, K. D. Shimizu, *Org. Chem. Front.* **2019**, *6*, 1266-1271.
- [20] M. Yamada, F. Tancini, M. Sekita, D. M. Guldi, C. Boudon, J.-P. Gisselbrecht, M. N. Alberti, W. B. Schweizer, F. Diederich, *Fullerenes, Nanotubes, Carbon Nanostruct.* **2014**, *22*, 99-127.
- [21] F. Ajamaa, T. M. F. Duarte, C. Bourgogne, M. Holler, P. W. Fowler, J.-F. Nierengarten, *Eur. J. Org. Chem.*, **2005**, 3766-3774.

RESEARCH ARTICLE

- [22] a) S. Aroua, Y. Yamakoshi, *J. Am. Chem. Soc.* **2012**, *134*, 20242-20245; b) S. Aroua, W. B. Schweizer, Y. Yamakoshi, *Org. Lett.* **2014**, *16*, 1688-1691.
- [23] a) M. Maggini, G. Scorrano, M. Prato, *J. Am. Chem. Soc.* **1993**, *115*, 9798-9799; b) M. Prato, M. Maggini, *Acc. Chem. Res.* **1998**, *31*, 519-526.
- [24] The free energies of activation for **1c** and **1h** were both calculated to be 63 kJ mol⁻¹ based on the Eyring equation and the coalescence temperature of their H^{Me} signals ($T_c = 323$ K) in CDCl₃.
- [25] O. Lukyanova, A. Kitaygorodskiy, C. M. Cardona, L. Echegoyen, *Chem. Eur. J.* **2007**, *13*, 8294-8301.
- [26] a) Y. Zhao, D. G. Truhlar, *Acc. Chem. Res.* **2008**, *41*, 157-167; b) Y. Zhao, D. G. Truhlar, *Theor. Chem. Acc.* **2008**, *120*, 215-241.
- [27] W. J. Hehre, R. Ditchfield, J. A. Pople, *J. Chem. Phys.* **1972**, *56*, 2257-2261.
- [28] M. Cossi, N. Rega, G. Scalmani, V. Barone, *J. Comput. Chem.* **2003**, *24*, 669-681.
- [29] a) Y. Umezawa, S. Tsuboyama, K. Honda, J. Uzawa, M. Nishio, *Bull. Chem. Soc. Jpn.* **1998**, *71*, 1207-1213; b) H. Suezawa, T. Yoshida, S. Ishihara, Y. Umezawa, M. Nishio, *CrystEngComm* **2003**, *5*, 514-518; c) M. Nishio, *CrystEngComm* **2004**, *6*, 130-158.
- [30] K. Wolinski, J. F. Hilton, P. J. Pulay, *J. Am. Chem. Soc.* **1990**, *112*, 8251-8260.
- [31] a) A. D. Becke, *Phys. Rev. A* **1988**, *38*, 3098-3100; b) A. D. Becke, *J. Chem. Phys.* **1993**, *98*, 5648-5652; c) C. Lee, W. Yang, R. G. Parr, *Phys. Rev. B* **1988**, *37*, 785-789.
- [32] Previous studies have suggested that the selected method is sufficiently accurate for reproducing the ¹H and ¹³C NMR chemical shifts of fullerenes and fullerene derivatives: a) G. Sun, M. Kertesz, *J. Phys. Chem. A* **2000**, *104*, 7398-7403; b) J. C. Duchamp, A. Demortier, K. R. Fletcher, D. Dorn, E. B. Iezzi, T. Glass, H. C. Dorn, *Chem. Phys. Lett.* **2003**, *375*, 655-659; c) M. Yamada, R. Ochi, Y. Yamamoto, S. Okada, Y. Maeda, *Org. Biomol. Chem.* **2017**, *15*, 8499-8503; d) M. Yamada, M. Takizawa, Y. Nukatani, M. Suzuki, Y. Maeda, *J. Org. Chem.* **2019**, *84*, 9025-9033.
- [33] M. Prato, T. Suzuki, F. Wudl, V. Lucchini, M. Maggini, *J. Am. Chem. Soc.* **1993**, *115*, 7876-7877.
- [34] C. Hansch, A. Leo, R. W. Taft, *Chem. Rev.* **1991**, *91*, 165-195.
- [35] R. Bosque, J. Sales, *J. Chem. Inf. Comput. Sci.* **2002**, *442*, 1154-1163.
- [36] E. V. Anslyn, D. A. Dougherty, *Modern Physical Organic Chemistry*, University Science Books, Herndon, **2005**.
- [37] L.-J. Riwar, N. Trapp, B. Kuhn, F. Diederich, *Angew. Chem.* **2017**, *129*, 11405-11410; *Angew. Chem. Int. Ed.* **2017**, *56*, 11252-11257.
- [38] C. A. Hunter, *Angew. Chem.* **2004**, *116*, 5424-5439; *Angew. Chem. Int. Ed.* **2004**, *43*, 5310-5324.

RESEARCH ARTICLE

Entry for the Table of Contents



Fullerene-based molecular torsion balance is constructed for investigating noncovalent arene–fullerene interactions for the first time. Results show that the interactions are weak but measurable. The linear correlation between the difference in the free energies of two well-defined conformers and the Hammett constants of the substituents on the arene moieties indicate that the electrostatic interactions contribute significantly to the overall interactions.